J. Exp. Biol. (1972), 56, 481–492
With 8 text-figures
Printed in Great Britain

DISTRIBUTION OF OXYGEN TENSION IN THE BLOOD AND WATER ALONG THE SECONDARY LAMELLA OF THE ICEFISH GILL

BY G. M. HUGHES

Research Unit for Comparative Animal Respiration, The University, Bristol, BS8 1UG

(*Received* 17 *September* 1971)

In spite of the extensive studies that have been made in recent years on the structure and function of gills, especially in fish, little is known about the O_2 tensions at different points along the exchange surface.

Although the terminal water and blood tensions have been measured for a number of fish (Stevens & Randall, 1967; Piiper & Baumgarten-Schumann, 1967, 1968; Holeton, 1970; Garey, 1967), investigation of this aspect of gill function is extremely difficult. Measurements of the tension at different points along the lamellar surfaces have been made only for the crab gill (Hughes, Knights & Scammell, 1969). A knowledge of the distribution of O_2 tensions along the exchange surface is important theoretically and also for practical use in relation to diffusing capacity etc. In many recent studies the term ΔP_G (Randall, Holeton & Stevens, 1967; Holeton, 1970; Jones *et al.* 1970) has been used as a measure of the effective O_2 tension difference. It assumes a linear relationship between gas tension and content, and that the difference between water and blood O_2 tensions is constant along the exchange surface. Piiper & Baumgarten-Schumann (1968) recognized this deficiency and applied a Bohr integration method to the dogfish gill.

In a recent analysis (Hughes & Hills, 1971) the distribution of O_2 tensions in the dogfish gill was calculated and plotted by a method which took into account the particular shape of the secondary lamellae and also the blood O_2 dissociation curve. The dogfish was convenient because CO_2 has relatively little effect on the O_2 dissociation curve. In many ways the antarctic fish which lack haemoglobin are even more ideal since complications due to the form of the O_2 dissociation curve are absent, which makes them suitable material for theoretical analyses on the influence of secondary lamellar shape. Gas tensions in the water and blood have been measured for the icefish (Holeton, 1970), and are combined with recent measurements of the secondary gill lamellae in this analysis.

MEANINGS OF SYMBOLS

$\dot{V}$ = volume of water passing across gills in unit time.
$\dot{Q}$ = volume of blood passing through gills in unit time.
S_w = solubility coefficient of O_2 in water.
S_b = solubility coefficient of O_2 in blood (= S_w in icefish).
P_{wi} = O_2 tension of water entering the gill.

P_{wo} = O_2 tension of water leaving the gill.
P_{aff} = O_2 tension in afferent blood, entering the gill.
P_{eff} = O_2 tension in efferent blood, leaving the gill.
p_w = O_2 tension of water at a particular point, x, along a secondary lamella.
p_b = O_2 tension in blood at x, along a secondary lamella.
C_a = O_2 content of afferent blood.
C_e = O_2 content of efferent blood.

MATERIALS AND METHODS

Specimens of *Chaenocephalus aceratus* were caught near the Signy Island laboratory of the British Antarctic Survey. They were used in laboratory experiments which included the measurement of O_2 tensions in the inspired and expired water, and in afferent and efferent blood under the conditions described by Holeton (1970). Gills of some of the fish used were brought to Bristol and their surface areas were measured using a method of weighted averages. It was shown that these areas were smaller than those previously measured (Hughes in Hughes & Shelton, 1962; Steen & Kruysse, 1966) and further investigation has suggested that the earlier specimens were not *Chaenocephalus aceratus* but another species of icefish, possibly *Pseudochaenichthys georgianus*. Profiles of individual secondary lamellae were taken and measurements were made of the cumulative surface area as described by Hughes (1970) (Figs. 1–3).

RESULTS

A. *Morphology of the secondary lamellae*

The surface areas of the gills and their component parameters are shown in Table 1, together with corresponding data from earlier measurements.

The most obvious differences are in the number of secondary lamellae per millimetre and the area of an average secondary lamella. Such marked differences strongly support the view that the earlier measurements were on a different species.

Table 1. *Gill area measurements for two specimens of* Chaenocephalus aceratus *brought from Signy Island by Dr G. F. Holeton*

		Filaments		Secondary lamellae			Gill areas	
Fish	Body wt (g)	Total number	Total length (mm)	No. on one side filament (mm)	Total number	Bilateral area of av. sec. lamella (mm^2)	Total area (mm^2)	Area/ body wt. (mm^2/g)
Chaenocephalus aceratus	860	1716	15,904	9·7*	308,537	0·300*	92,561	107·6
	1456	1744	21,633	9·6*	415,353	0·443*	184,002	126·4
?*Chaenocephalus*† sp.	750	1452	17,378	12	417,072	0·80	333,657	444·9
	790	1564	15,386	12	369,264	0·84	310,182	392·6

* Weighted averages. † After G. M. Hughes (1962)

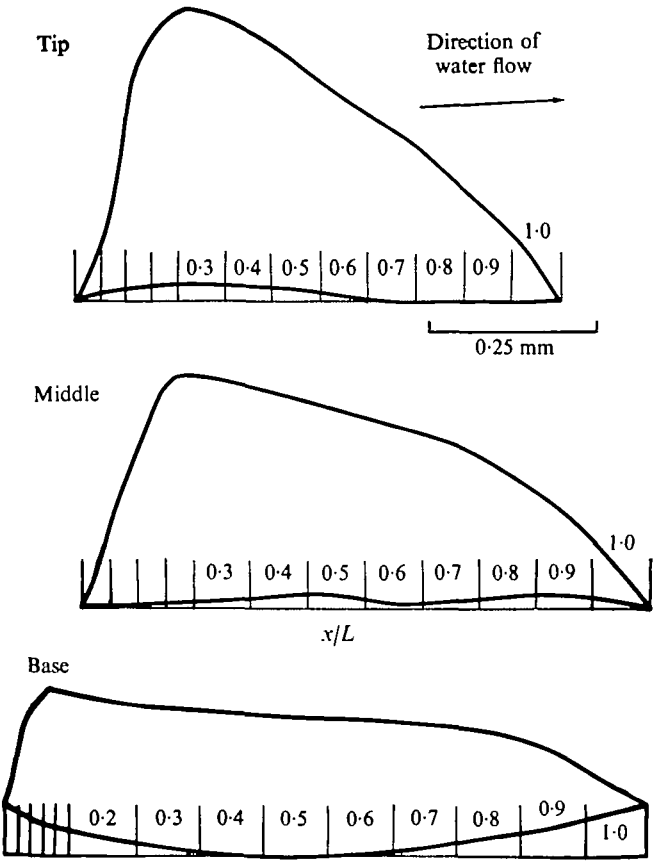

Fig. 1. Profiles of secondary lamellae from the tip, middle and base of filament from the gills of *Chaenocephalus aceratus*

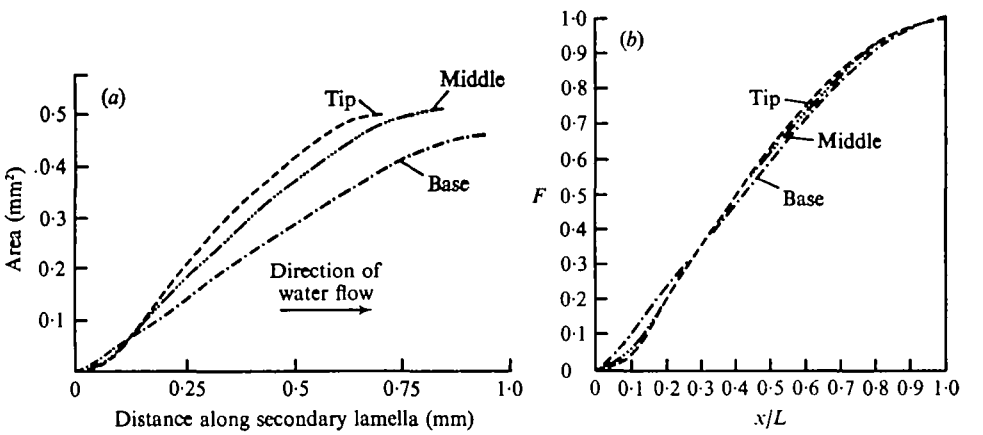

Fig. 2. Cumulative areas of the secondary lamellae from the gills of *C. aceratus*. In *a* absolute values of area (mm^2) are plotted against path length (mm), whereas in *b* fractional values of area (*F*) are plotted against fractional path length (*x*/*L*).

From Figs. 1 and 2*a* it is clear that although the bilateral surface area may not differ for secondary lamellae from the tip or middle of a filament, there are marked differences in their form, as shown by plotting cumulative area against water-path length. However, the same data plotted so as to cancel out differences in absolute dimensions (Fig. 2*b*), shows that secondary lamellae from the tip and middle of a filament have very similar relationships between cumulative area and fractional path length. Secondary lamellae from the base of the filament, however, are somewhat different in that their cumulative area increases more rapidly from the point of water entry and is added to at a constant rate over more than 95% of the remaining path length. Cumulative area can also be plotted in the direction of blood flow as is done below (figs. 3 and 5) because this will not change from co-current to counter flow.

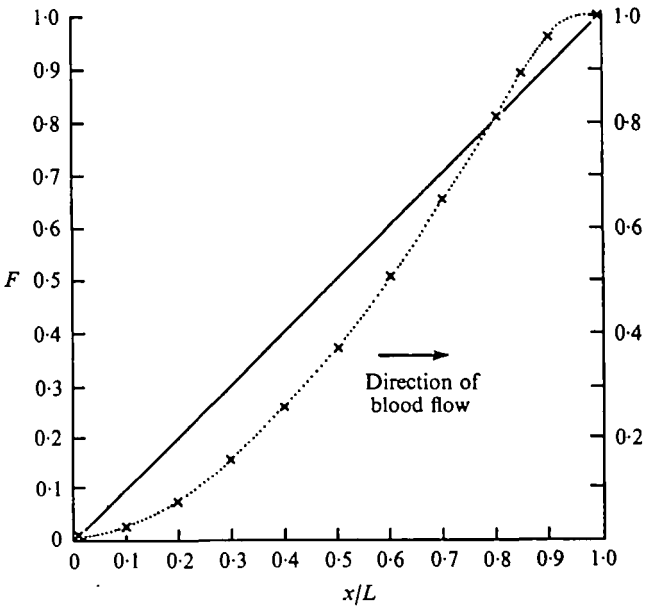

Fig. 3. Cumulative area for a secondary lamella from the tip of a filament (...) plotted in the direction of blood flow. The full line shows the plot for a secondary lamella of rectangular shape (1 in Fig. 8). Fractional path length is also given in the same direction.

B. *Analysis of O_2 tension distribution along a secondary lamella*

The method adopted is the same as that developed by Hughes & Hills (1971) for the dogfish. Essentially this consists in dividing the known overall change in blood O_2 tension into a convenient number of sections, in this case 11 (column A, Table 2). The corresponding percentage saturation of the blood is calculated assuming a linear relationship between tension and content (column B). From the available data and the mass-balance equation

$$\dot{V}S_w\,(P_{wi}-P_{wo}) = \dot{Q}\,(C_e-C_a),$$

it follows that

$$\dot{Q}/\dot{V}S_w = \frac{(P_{wi}-P_{wo})}{(C_e-C_a)}.$$

(Note that in this particular case the capacity rate ratio (Hughes, 1964), $\dot{Q}S_b/\dot{V}S_w$, would have been the appropriate constant.) Inserting data based on that summarized

Table 2*a*. *Typical computation for the icefish secondary lamella*

	p_b (A)	C (B)	$C-C_a$ (D)	$P_{wi}-p_w$ (E)	p_w (G)	p_w-p_b (H)	$1/(p_w-p_b)$ (I)	F (J)	x/L (K)
Source	—	Blood	B−16·7	0·474D	150−E	G–A	1/H	Fig. 4	Fig. 5
	—	Curve	C_a=16·7		P_{wi} = 150	—	—	—	—
Units ...	mmHg	% sat.	% sat.	mmHg	mmHg	mmHg	$(mmHg)^{-1}$	O	O
Flow ...	—	—	—	—	—	Co-current	—	—	—
	25	16·7	0·0	0·0	150·00	125·00	0·0080	0·000	1·000
	30	20·0	3·3	1·56	148·44	118·44	0·0084	0·012	0·925
	40	26·7	10·0	4·74	145·26	105·26	0·0095	0·045	0·861
	50	33·3	16·6	7·87	142·13	92·13	0·0109	0·079	0·805
	60	40·0	23·3	11·04	138·96	78·96	0·0127	0·122	0·746
	70	46·7	30·0	14·22	135·78	65·78	0·0152	0·171	0·693
	80	53·3	36·6	17·35	132·65	52·65	0·0190	0·226	0·625
	90	60·0	43·3	20·52	129·48	39·48	0·0253	0·301	0·560
	100	66·7	50·0	23·70	126·30	26·30	0·0380	0·410	0·466
	110	73·3	56·6	26·83	123·17	13·17	0·0759	0·590	0·335
	120	80·0	63·3	30·00	120·00	0·00		1·000	0·000

Table 2*b*

	p_b (A)	C (B)	C_a-C (L)	$P_{wi}-p_w$ (M)	p_w (N)	p_w-p_b (Q)	$1/(p_w-p_b)$ (R)	F (S)	x/L (T)
Source	—	Blood	80−B	0·474L	150−M	N–A	1/Q	Fig. 4	Fig. 5
	—	Curve	C_a = 80		P_{wi} = 150	—	—	—	—
Units ...	mmHg	% sat.	% sat.	mmHg	mmHg	mmHg	$(mmHg)^{-1}$	O	O
Flow ...	—	—	—	—	—	Counter-current	—	—	—
	25	16·7	63·3	30·04	119·96	94·96	0·0105	0·000	1·000
	30	20·0	60·0	28·44	121·56	91·56	0·0109	0·030	0·890
	40	26·7	53·3	25·26	124·74	84·74	0·0118	0·094	0·770
	50	33·3	46·7	22·14	127·86	77·86	0·0128	0·171	0·696
	60	40·0	40·0	18·96	131·04	71·04	0·0141	0·245	0·615
	70	46·7	32·3	15·31	134·69	64·69	0·0155	0·349	0·520
	80	53·3	26·7	12·66	137·34	57·34	0·0174	0·434	0·458
	90	60·0	20·0	9·48	140·52	50·52	0·0198	0·540	0·373
	100	66·7	13·3	6·30	143·70	43·70	0·0229	0·665	0·289
	110	73·3	6·7	3·18	146·82	36·82	0·0272	0·808	0·195
	120	80·0	0·0	0·00	150·00	30·00	0·0333	1·00	0·000

by Holeton (1970), i.e. P_{wi} = 150 mm; P_{wo} = 120 mm; P_{aff} = 25 mm; P_{eff} = 120 mm this ratio is 0·474. This constant can now be inserted in equations for co-current and counter-current flow, enabling $(P_{wi}-p_w)$ to be calculated and hence the water O_2 tensions (p_w) which correspond to the chosen blood O_2 tensions at different positions along the secondary lamella. From this data and a plot (Fig. 4) of $1/(p_w-p_b)$ against O_2 tensions between P_{wo} and P_{wi}, it is possible to obtain values for the function F, by graphical integration:

$$F = \int_{p_w}^{P_{wi}} \frac{dp_w}{p_w-p_b} \Big/ \int_{P_{wo}}^{P_{wi}} \frac{dp_w}{p_w-p_b}.$$

This fractional change is effectively a measure of the area necessary for O_2 transfer assuming either co-current or counter-current flow, i.e. the greater the area beneath this curve (Fig. 4) the greater the area required for gas exchange. In Fig. 4 it is shown that the total area under the curve for co-current is 91·58 as against 52·96 for counter-current flow and from which the fractional areas may be derived (I in Table 3) at

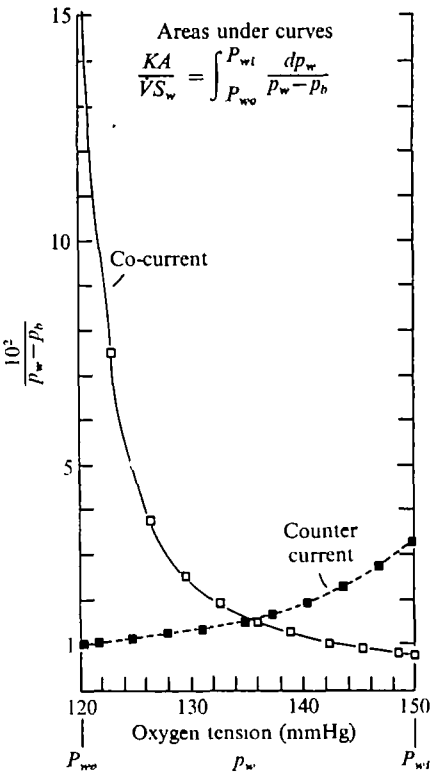

Fig. 4. Plots of $1/(p_w - p_b)$ against p_w which permits the calculation of

$$\int_{P_{wo}}^{P_{wi}} \frac{dp_w}{p_w - p_b}$$

by graphical integration. Column I versus G and R versus N in Table 2.

Table 3. *Result of graphical integration of curves plotted in Fig. 4 giving values of (I) which are expressed as fractions in column (F)*

	Co-current		Counter-current	
p_w	*I*	*F*	*I*	*F*
120	91·58	1·000	0·00	0·000
123	55·33	0·604	3·22	0·061
126	38·73	0·423	6·70	0·127
129	29·04	0·317	10·42	0·197
132	22·07	0·241	14·47	0·273
135	16·68	0·182	18·90	0·375
138	12·33	0·135	23·82	0·450
141	8·58	0·094	29·40	0·555
144	5·32	0·058	35·94	0·679
147	2·48	0·027	43·68	0·825
150	0·00	0·000	52·95	1·000

$$I = \int_{p_w}^{150} \frac{100\, dp_w}{p_w - p_b} = \begin{matrix} 91{\cdot}58 \\ \text{or} \\ 52{\cdot}95 \end{matrix}$$

$$F = \frac{I}{91{\cdot}58} \quad \text{or} \quad \frac{I}{52{\cdot}95}$$

different values of p_w between P_{wo} and P_{wi}. Having obtained values for F from both morphological and functional plots, it is possible to read off the corresponding fractional path length (x/L) along the secondary lamella for p_w and hence p_b (Fig. 5). When

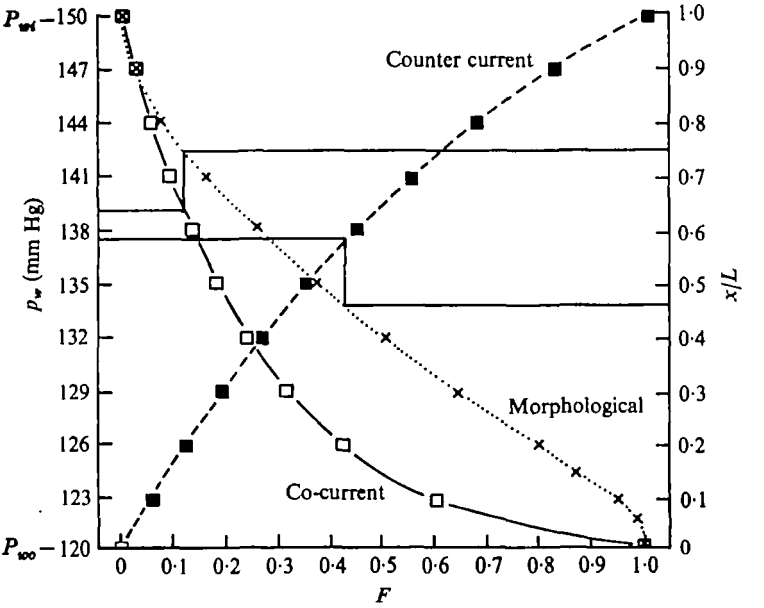

Fig. 5. Morphological plot of F (cumulative area in direction of blood flow) of the secondary lamella against the fractional path length (x/L). The functional plot of F versus water O_2 tension is also shown for co-current and counter-current flows. The way in which these plots enable p_w and p_b to be matched against x/L is indicated for one point for each type of flow.

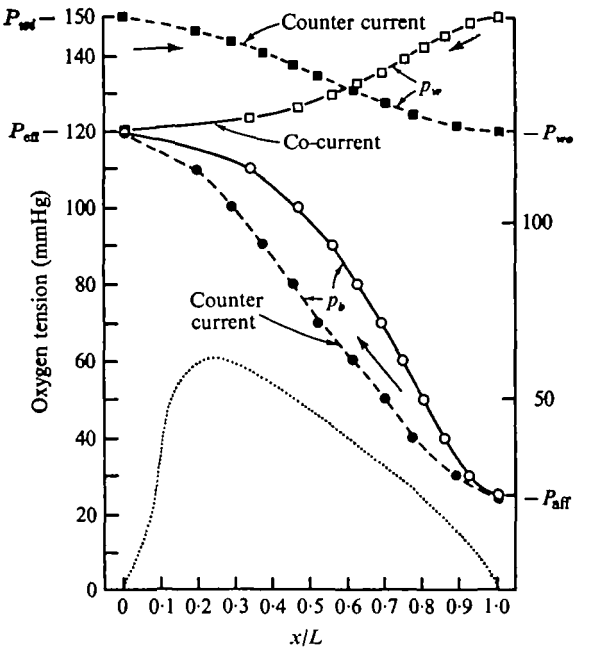

Fig. 6. Distribution of O_2 tensions in blood and water along a secondary lamella for counter-current and co-current flow.

plotted out these values give the final graph showing the distribution of O_2 tensions in the water and blood for co-current and counter-current flows across the chosen secondary lamella profile.

From this plot (Fig. 6) it is clear that for co-current flow the gas tensions approach one another asymptotically so that the difference in O_2 tension between water and blood is very great to begin with but finally becomes zero. Correspondingly $1/(p_w - p_b)$ approaches infinity (Fig. 4). With counter-current flow, however, there is always a significant difference between the water and blood O_2 tensions. The usual method of calculation:

$$\Delta P_G = \tfrac{1}{2}[(P_{wi} - P_{eff}) + (P_{wo} - P_{aff})]$$

assumes straight lines between P_{wi} and P_{wo}, and between P_{aff} and P_{eff} which is clearly a gross approximation. A better method of estimating ΔP_G is available from these curves by calculating the mean of the integrated area of the O_2 differential between the water and blood across the whole secondary lamella. However, use of the arithmetic mean is only valid if the two curves are parallel, which is clearly not true. Except under the special conditions where ΔP_G is appropriate, it would seem preferable to use the log mean P_{O_2} gradient (Hughes, 1972), i.e.

$$\frac{(P_{wi} - P_{eff}) - (P_{wo} - P_{aff})}{\log_e \dfrac{(P_{wi} - P_{eff})}{(P_{wo} - P_{aff})}}.$$

C. *The effect of secondary lamella shape on the O_2 tension distribution*

Because the blood O_2 dissociation curve is not a complicating factor, the icefish provides a suitable model for investigating the effects of different shapes of secondary lamellae on the O_2 tension distribution. The profiles shown in Fig. 7 have been

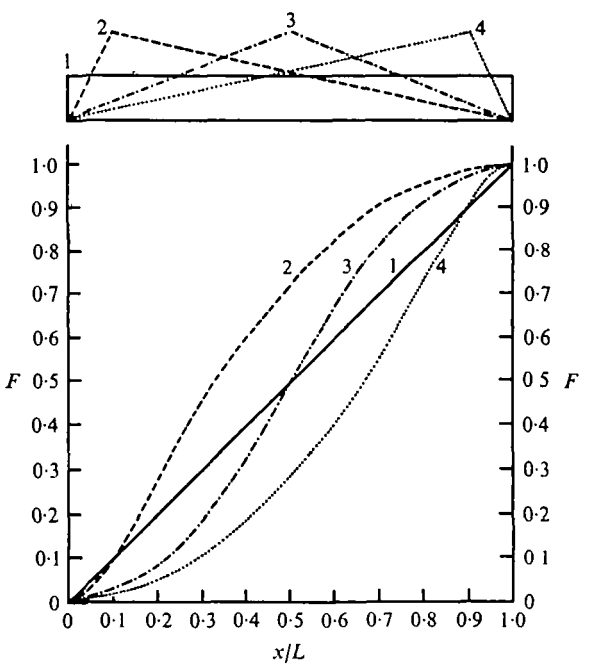

Fig. 7. Model profiles for secondary lamellae together with their appropriate cumulative areas in the direction of counter-current water flow.

used to plot out cumulative areas along the fractional path length. These morphological plots of F against x/L were used together with data for the terminal water and blood O_2 tensions in the same way as described for counter-current flow across an actual secondary lamella and are shown in fig. 8.

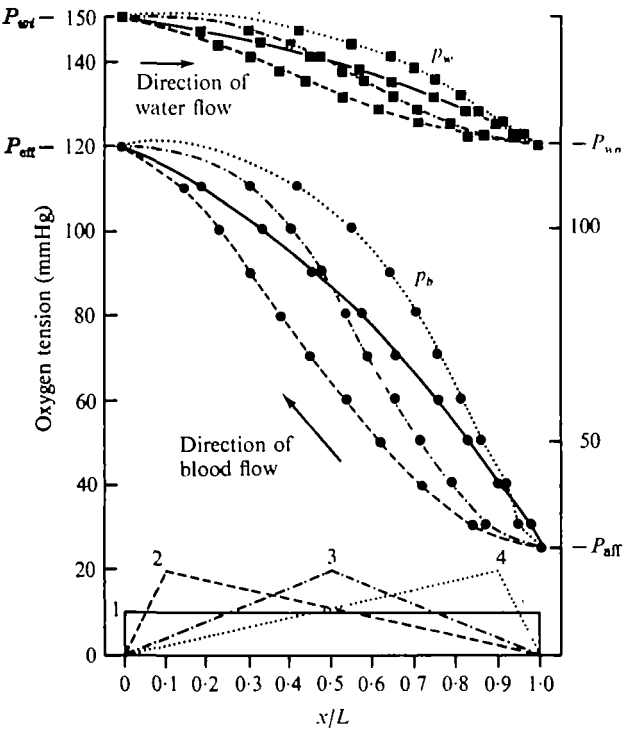

Fig. 8. Distribution of p_w and p_b during counter-current flows for the same four profiles used in Fig. 7 indicated by different types of dotted and dashed lines.

For the simple rectangular profile (1), the blood and water tensions are slightly greater than those obtained by connecting directly P_{wi} with P_{wo} and P_{aff} with P_{eff}. For a profile in which the major part of the area comes early in the water path length (2), p_w falls more rapidly than in the other cases and correspondingly p_b increases less rapidly at the afferent end because this particular model has the least exchange area in this region of the path length.

Calculations based on secondary lamellae from the tip or middle of a filament show tension changes which lie somewhat between profiles 2 and 3 as would be expected from their geometry. The advantages of a shape such as that in profile 2 is that it ensures that the maximum exchange area is in the region where the difference in O_2 tensions of water and blood is smaller and vice versa. Hence this particular arrangement maintains the greatest tension differential between water and blood throughout their passage across the gill.

DISCUSSION

The measurements made on the gills of *Chaenocephalus aceratus* confirm the generalization made from the previous specimens of icefish that the sieve will provide

relatively little resistance to water flow (Hughes, 1966). The smaller gill area of these specimens is presumably an interspecific difference. From the data reported here and other specimens (G. F. Holeton, personal communication), it seems that the weight-specific gill area remains constant at all body sizes.

Because of its lack of haemoglobin the icefish is useful in several theoretical calculations. It illustrates, for example, the value of the concept of effectiveness as against utilization as a measure of the performance of a gill gas exchanger. This is especially so if one remembers that from a homeostatic point of view it is the condition of the blood leaving the gill which is so important (Hughes, 1964).

Utilization of O_2 in water,

$$U = \frac{P_{wi} - P_{wo}}{P_{wi}} = \frac{150 - 120}{150} = 20\%.$$

Effectiveness of O_2 removal from water,

$$E_w = \frac{P_{wi} - P_{wo}}{P_{wi} - P_{aff}} = \frac{150 - 120}{150 - 25} = \frac{30}{125} = 24\%,$$

but E_b = effectiveness of oxygen uptake by the blood

$$= \frac{P_{eff} - P_{aff}}{P_{wi} - P_{aff}} = \frac{120 - 25}{150 - 25} = \frac{95}{125} = 76\%.$$

The same is also true of a rainbow trout when the haemoglobin has been combined with carbon monoxide (Table 4).

Table 4. *Percentage utilization* (U), *effectiveness of* O_2 *removal from water* (E_w) *and of* O_2 *uptake by blood* (E_b) *for icefish and rainbow trout* (*data from Holeton* (1970, 1971)).

	U	E_w	E_b
Icefish	20	24	76
Rainbow trout			
Normal	50	59·1	52
CO-treated	16·5	17·9	69·3

Thus the gill is very effectively carrying out its function of oxygenating the blood, although it does not seem very efficient as measured by its utilization of O_2 in the water. The analysis presented in this paper indicates that an important factor in maintaining this performance is not only the area of the gas-exchange surface but also its particular shape. The shape most commonly found and used here seems to be designed to maintain a high difference in gas tension between the water and blood throughout their passage over the exchange surface.

From the measurements available, it seems almost certain that counter-current flow is normally present, and these calculations have been based on this assumption.

Because of the linear relationship between blood and water O_2 tensions in icefish, it can be shown (B. A. Hills and G. M. Hughes, unpublished), that

$$\frac{\dot{V}_{O_2}}{A} \propto a p_w.$$

Hence, a greater total amount of O_2 will be transferred for a given area of exchange surface if a larger proportion (a) of the total secondary lamellar area (A) is in contact

with water of the highest O_2 tensions. Further analysis of gas transfer across secondary lamellae must take into account the differences in path length of the water flowing at different levels of the secondary lamella rather than assume that all the water remains within the profile boundary, as is true for the blood.

A further limitation of this type of analysis relates to the basic experimental data used in the calculations (i.e. values of P_{wi}, P_{wo}, P_{aff} and P_{eff}). Although it would be extremely difficult to obtain true values for P_{aff} and P_{eff} of individual secondary lamellae, this should be possible for P_{wi} and P_{wo} and hence some of the dilution effects of water shunted between the filament tips could be assessed. Before such analyses can be expanded to the whole of the gill system a great deal needs to be learned about different degrees of recruitment on both sides of the exchanger and consequent ventilation/perfusion inequalities (Hughes, 1972).

SUMMARY

1. Measurements of the gill area of two specimens of *Chaenocephalus aceratus* indicate that the resistance to water flow and overall exchange area are even less than had been supposed from work with other icefish.

2. Measurements of the oxygen tensions in the water and in blood entering and leaving the gills are used to determine the expected distribution of O_2 tensions along a typical secondary lamella profile. The advantage of counter-current over co-current flow is clearly indicated by such analyses.

3. The absence of complications due to the O_2 dissociation curve of the blood facilitates an extension of the analysis to different theoretical secondary lamellar profiles. It is shown that profiles similar to those usually found in fish gills are more efficient in maintaining O_2 transfer.

4. Although the percentage utilization of O_2 in the water passing through the gills is relatively low, the effectiveness of oxygenating the blood is very high in the icefish gill.

This work was supported by a grant from the Natural Environment Research Council. I wish to thank Dr. G. F. Holeton for carrying out the O_2 measurements and bringing back the gill material from Signy Island. I also enjoyed valuable discussion with Dr Brian Hills.

REFERENCES

GAREY, W. F. (1967). Gas exchange, cardiac output and blood pressure in free swimming carp (*Cyprinus carpio*). Dissertation, State University of New York at Buffalo, Buffalo, N.Y.

HOLETON, G. F. (1970). Oxygen uptake and circulation by a haemoglobinless Antarctic fish (*Chaenocephalus aceratus* Lonnberg) compared with three red-blooded Antarctic fish. *Comp. Biochem. Physiol.* **34**, 457–71.

HOLETON, G. F. (1971). Oxygen uptake and transport by the rainbow trout during exposure to carbon monoxide. *J. exp. Biol.* **54**, 239–54.

HUGHES, G. M. (1964). Fish respiratory homeostasis. *Symp. Soc. exp. Biol.* **18**, 81–107.

HUGHES, G. M. (1966). The dimensions of fish gills in relation to their function. *J. exp. Biol.* **45**, 177–95.

HUGHES, G. M. (1970). Morphological measurements on the gills of fishes in relation to their respiratory function. *Folia morph., Prague*, **18**, 78–95.

HUGHES, G. M. (1972). Morphometrics of fish gills. *Resp. Physiol.* (in the Press).

HUGHES, G. M. & HILLS, B. A. (1971). Oxygen tension distribution in water and blood at the secondary lamella of the dogfish gill. *J. exp. Biol.* **55**, 399–408.

HUGHES, G. M., KNIGHTS, B. & SCAMMELL, C. A. (1969). The distribution of P_{O_2} and hydrostatic pressure changes within the branchial chambers in relation to gill ventilation of the shore crab *Carcinus maenas* L. *J. exp. Biol.* **51**, 203–30.

HUGHES, G. M. & SHELTON, G. (1962). Respiratory mechanisms and their nervous control in fish. *Advances in Comparative Physiology and Biochemistry* (ed. O. Lowenstein) **1**, 275–364. Academic Press Inc.

JONES, D. R., RANDALL, D. J. & JARMAN, G. M. (1970). A graphical analysis of oxygen transfer in fish. *Resp. Physiol.* **10**, 285–98.

PIIPER, J. & SCHUMANN, D. (1967). Efficiency of O_2 exchange in the dogfish *Scyliorhinus stellaris*. *Resp. Physiol.* **2**, 135–48.

PIIPER, J. & BAUMGARTEN-SCHUMANN, D. (1968). Effectiveness of O_2 nd CO_2 exchange in the gills of the dogfish (*Scyliorhinus stellaris*). *Resp. Physiol.* **5**, 338–49.

RANDALL, D. J., HOLETON, G. F. & STEVENS, E. D. (1967). The exchange of oxygen and CO_2 across the gills of rainbow trout. *J. exp. Biol.* **46**, 339–48.

STEEN, J. B. & KRUYSSE, A. (1964). The respiratory function of teleostean gills. *Comp. Biochem. Physiol.* **12**, 127–42.

STEVENS, E. D. & RANDALL, D. J. (1967). Changes of gas concentrations in blood and water during moderate swimming activity of rainbow trout. *J. exp. Biol.* **46**, 329–37.